

# Effect of processing methods and functional groups on the properties of multi-walled carbon nanotube filled poly(dimethyl siloxane) composites

K. T. S. Kong · M. Mariatti · A. A. Rashid ·  
J. J. C. Busfield

Received: 9 August 2011 / Revised: 30 November 2011 / Accepted: 22 May 2012 /  
Published online: 3 June 2012  
© Springer-Verlag 2012

**Abstract** Pristine and functionalized multi-walled carbon nanotubes (MWCNTs) filled poly(dimethyl siloxane) (PDMS) composites were produced by two different methods, namely the solution mixing method and the mini-extruder method. The composites produced using the mini-extruder exhibit relatively higher tensile strength and higher thermal conductivity due to better nanotubes dispersion. On the other hand, the composites prepared via solution mixing have higher electrical conductivity and better thermal stability due to the high aspect ratio of nanotubes. Scanning electron micrographs of composites fracture surface revealed that composites produced by mini-extruder resulted shorter nanotube length, thus lowering the aspect ratio of MWCNTs. In general, functionalization of nanotubes increases the tensile strength, thermal conductivity, and thermal stability of the PDMS composites due to the improved interfacial adhesion and nanotubes dispersion.

**Keywords** Tensile strength · Electrical conductivity · Thermal analysis · Mini-extruder · Solution mixing

## Introduction

The discovery of carbon nanotubes (CNTs) by Ijima in 1991 [1] drew enormous interest from researchers worldwide owing to their exceptional properties such as high thermal and electrical conductivity, excellent mechanical properties, and good thermal stability [2, 3]. Due to these unique properties, CNTs are being increasingly

---

K. T. S. Kong · M. Mariatti (✉) · A. A. Rashid  
School of Materials and Mineral Resources Engineering, Universiti Sains Malaysia,  
14300 Nibong Tebal, Penang, Malaysia  
e-mail: mariatti@eng.usm.my

J. J. C. Busfield  
Department of Materials, Queen Mary University of London, London E1 4NS, UK

used as fillers in polymer composites for various applications, such as electrostatic discharge material, electromagnetic–radio frequency interference protection [4], and thermal interface materials [5]. Poly(dimethyl siloxane) (PDMS) is a type of silicone rubber with outstanding properties which includes high elasticity, good tear strength, resistance to chemical, thermal shocks, and extreme temperatures [6, 7]. The addition of CNTs into PDMS matrix improves the mechanical, electrical, and thermal properties of the composites. Wu et al. [7] reported that the elastic modulus, storage modulus, and hardness of PDMS/CNT nanocomposite increases when 2 wt% CNTs are added into the PDMS matrix. In a separate work, Hong et al. [6] revealed that the thermal conductivity of PDMS/CNT nanocomposite increases with CNT loading.

Although previous works have shown properties improvement with the addition of CNTs in PDMS nanocomposite, the true potential of CNTs as fillers is limited and cannot be maximized because the CNTs are highly entangled. The high degree of entanglement is partly due to the high aspect ratio of CNTs, as well as the van der Waals interactions among them. Processing of CNT/polymer composites poses great challenges, primarily the non-uniform dispersion of CNTs in polymer matrix and poor interfacial adhesion between CNTs and polymer matrix [8, 9]. A great number of studies have been devoted to improving dispersion of CNTs in polymer matrix and interfacial adhesion between CNTs and polymers. Various processing techniques such as solution mixing [10] and melt compounding using mini-extruder [11] were used with the intention to improve dispersion and reinforcing efficiency of CNTs in polymer. A common method to improve interfacial adhesion between CNTs and polymer matrix is by introducing functional groups on the surface of the CNTs, which can provide multiple bonding sites to the polymeric matrix [9]. This can be done via treatments using silane [3, 12], amine [8], fluorine [13], and oxidation in acid solution [14].

While there have been various studies on the effect of different dispersion states and parameters on the properties of CNTs polymer composites [6, 15, 16], to the best of our knowledge, minimal research has been conducted on the combination effect of processing methods and functionalized fillers on the properties of PDMS composites filled with multi-walled carbon nanotubes (MWCNTs). The current work aims to compare the properties of PDMS/MWCNT composites produced by two different methods: solution mixing and shear mixing via mini-extruder. Solution mixing is a common, low cost and widely used method [17], whereas processing of PDMS composites using mini-extruder is less common. The effect of nanotube functionalization (–OH and –COOH group) on the properties of PDMS/MWCNT composites is also investigated in this study.

## Materials and methods

### Materials

PDMS (Sylgard 182 Silicone Elastomer) consisting of a base elastomer (Part A) and a curing agent (Part B) was purchased from Dow Corning, USA. The ratio of Part A

to Part B is 10:1. Pristine MWCNTs (MWCNT-p) 40–60 nm in diameter and 1–2  $\mu\text{m}$  in length, of 97 % purity, were purchased from Shenzhen Nanotech Port Co. Ltd., China. MWCNT-OH and MWCNT-COOH, both 30–50 nm in diameter and 0.5–2  $\mu\text{m}$  in length, of 95 % purity, were purchased from Nanostructured and Amorphous Materials, Inc., USA. The solvent used to disperse the MWCNTs was toluene (99.9 %) purchased from J.T. Baker.

#### Fabrication of PDMS/MWCNT composites via solution mixing method

For each type of nanotubes (MWCNT-p, MWCNT-OH, and MWCNT-COOH), composites with loadings of 1, 2, 3, and 4 wt% were produced. The parameters used in this method were based on previous work [5] and were further optimized to obtain the best result. The MWCNTs were first dispersed in 25 ml of toluene and sonicated in an ultrasonic bath for 1 h to achieve uniform dispersion. Part A of the PDMS was then added to the suspension of MWCNTs and toluene. The mixture was mechanically stirred for 1.5 h at 400 rpm and 70 °C to evaporate the toluene. After the mixture was cooled to room temperature, Part B was added and the mixture (Part A, Part B, and MWCNTs) was mechanically stirred for 10 min at 800 rpm and room temperature. The mixture was cast onto a 1.5 and 0.1 mm mold, respectively, followed by degassing under vacuum for 1 h before being cold compressed for 1 min. Finally, the compressed mixture was cured in an oven at 150 °C for 2 h.

#### Fabrication of PDMS/MWCNT composites using mini-extruder

The parameters used in this method were optimized from a series of experimental trial runs. MWCNTs were mixed with Part A (PDMS) using a mini-extruder for 10 min at room temperature. The model of mini-extruder used was DSM Research 15 ml Micro-Compounder, supplied by DSM Research, Netherlands. Screw rotating speed was set to 200 rpm. Part B was then added to the mini-extruder and was further mixed for 10 min at room temperature using the same rotating speed. The mixture was then extruded out onto a 1.5 and 0.1 mm mold plate, and subsequently degassed in vacuum for 1 h. The mixture was simultaneously pressed and cured at 150 °C for 2 h using a hot press.

#### Characterization of MWCNT fillers and PDMS/MWCNTs composites

The surface morphology of the MWCNTs was observed using the JEOL-2010 high-resolution transmission electron microscope. Raman spectra of the MWCNTs were collected with Jobin-Yvon HR 800 UV Raman spectroscope. Fourier Transform Infrared (FTIR) analysis was performed using the Perkin Elmer FTIR at room temperature. The viscosity of the uncured mixture (PDMS and MWCNTs) during mixing via mini-extruder was obtained directly from the equipped software, while for solution mixing, the viscosity was determined with Brookfields DV-II + viscometer. Dispersion of MWCNT in PDMS was observed using Olympus BX41TF optical microscope. Tensile test was conducted with an Instron 3366 universal testing machine using a crosshead speed of 500 mm/min. Samples were

cut into dumbbell shape according to the dimensions of Die C in ASTM D412. The fracture surface of the composites was observed with the FEI Quanta 3D environmental scanning electron microscope. The thermal conductivity of the composites was obtained using the hot disk thermal constant analyzer (TPS 2500S). The electrical conductivity of the composites was measured with Advantest R8340 ultra-high resistance meter using a constant voltage of 500 V. Thermogravimetric analysis (TGA) was conducted using Perkin Elmer's Pyris<sup>TM</sup> 6 TGA, heating from room temperature to 800 °C (heating rate: 10 °C/min) under nitrogen atmosphere to study the thermal stability of the composites.

## Results and discussion

### MWCNTs surface morphology

The microstructures of pristine MWCNTs and functionalized MWCNTs are shown in Fig. 1. Figure 1a shows that the wall surface of the pristine MWCNT-p is smooth and no extra phase is present. In contrast, the surfaces for both functionalized MWCNTs are heterogeneous and rough, as seen in Fig. 1b, c. This is due to acidic etching of the nanotube surfaces during chemical (acid) treatment to induce the functional groups [18].

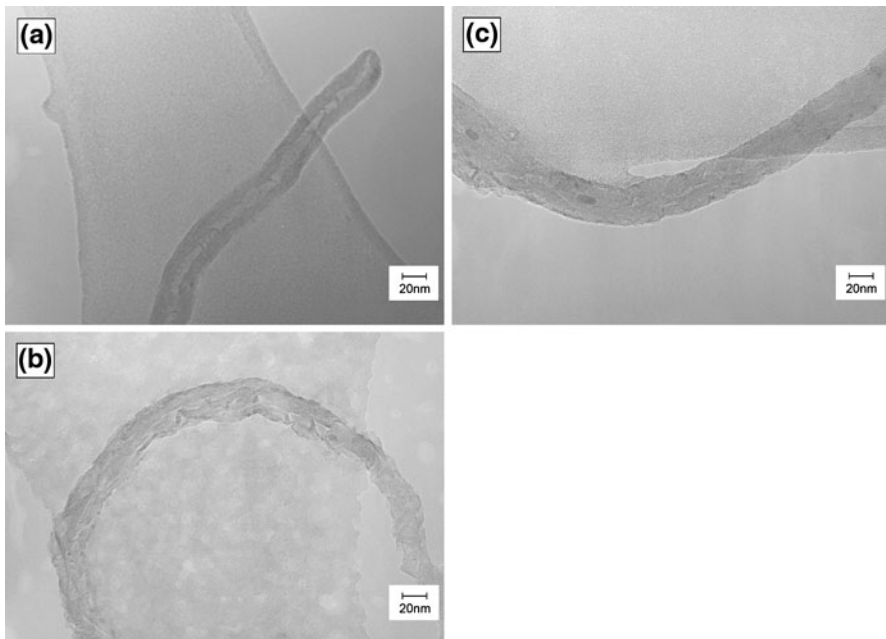


**Fig. 1** TEM images of **a** pristine MWCNT, **b** MWCNT-OH, and **c** MWCNT-COOH

## Raman spectroscopy analysis

The Raman spectra of pristine and functionalized MWCNTs are shown in Fig. 2. The MWCNTs display two characteristic peaks at approximately 1,340 and 1,570  $\text{cm}^{-1}$ , termed as *D*-band and *G*-band, respectively. The *G*-band relates to the structural intensity of the  $sp^2$ -hybridized carbon atoms of CNTs, whereas the *D*-band reflects disorder-induced carbon atoms resulting from the defects in CNTs and their ends [9, 19]. The higher *D*-band intensity and the lower *G*-band to *D*-band ratio ( $I_G/I_D$ ) of both MWCNT-OH and MWCNT-COOH indicate a high degree of disorder and the presence of defects on the surface of the functionalized CNT resulting from chemical modification [9].

## FTIR spectroscopy analysis

The FTIR spectrums of the MWCNTs studied (after smoothing and baseline correction) are shown in Fig. 3. The MWCNT-p spectrum shows only one weak peak at the wavelength 3,468  $\text{cm}^{-1}$ , which is assigned to hydroxyl groups. This peak could be due to absorbed moisture attached to the nanotubes [20]. The spectrum of MWCNT-OH shows three different peaks. The peak detected at 3,415  $\text{cm}^{-1}$ , which is also assigned to hydroxyl groups and attributed to stretching vibration of O–H, has higher and broad absorbance intensity as compared to MWCNT-p. The other two peaks detected at 1,021 and 1,444  $\text{cm}^{-1}$  are attributed to stretching vibration of C–OH and bending vibration of O–H, respectively. These observed peaks indicate that the –OH functional groups are present on the surface of nanotubes [21]. The MWCNT-COOH spectrum shows four characteristic peaks at 1073, 1428, 1737, and 3408  $\text{cm}^{-1}$ . The peaks at 1073, 1428, and 3408  $\text{cm}^{-1}$  are

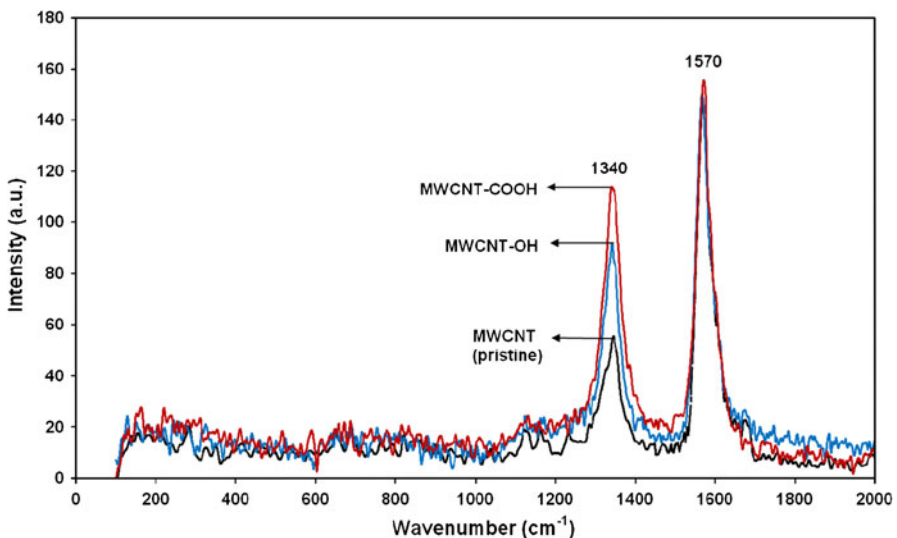


**Fig. 2** Raman spectra of pristine and functionalized MWCNTs

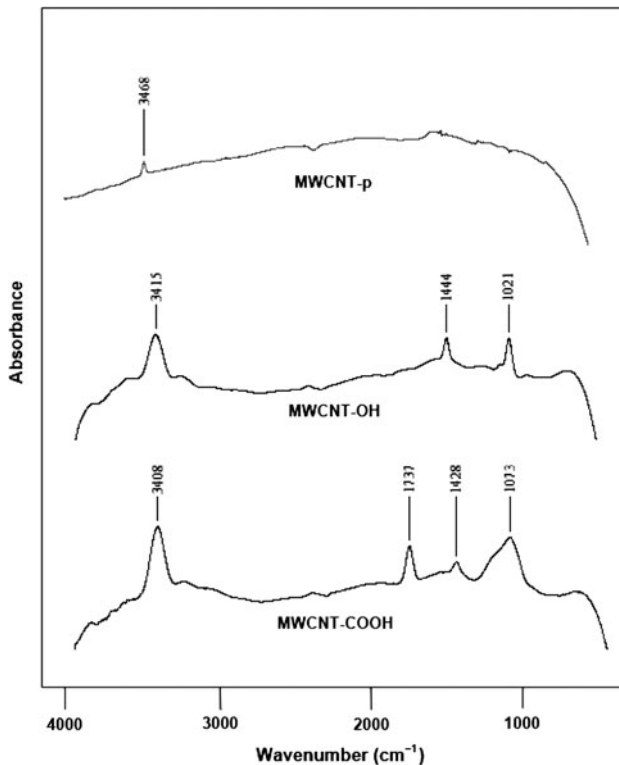


**Fig. 3** FTIR spectra of pristine and functionalized MWCNTs

attributed to C–OH stretch, O–H bend, O–H stretch, respectively, which is similar to the ones observed in MWCNT-OH. The peak at  $1,737\text{ cm}^{-1}$  is attributed C=O stretch, indicating the presence of carboxyl groups.

#### Dispersion of MWCNTs in PDMS

Figure 4 presents the transmission mode optical microscope digital micrographs of 4 wt% MWCNTs composites produced by mini-extruder (Fig. 4a–c) and solution mixing method (Fig. 4c–e), illustrating the overall distribution and dispersion of MWCNTs in PDMS matrices. The nanotubes are represented as black-colored area, while the PDMS polymer is represented as white-colored area. From Fig. 4a, it can be seen that the black area and white area are well distributed although some black spots can also be seen. On the other hand, many large black spots are observed in Fig. 4d, indicating the presence of large nanotubes agglomerates and clusters. From both micrographs, it can be deduced that composites produced by mini-extruder have relatively better dispersion of nanotubes in PDMS matrix.

Functionalization of MWCNTs can greatly affect the dispersion of nanotubes in PDMS. It is evident that functionalized MWCNTs, both MWCNT-OH (Fig. 4b, e) and MWCNT-COOH (Fig. 4c, f) are relatively much better dispersed and distributed



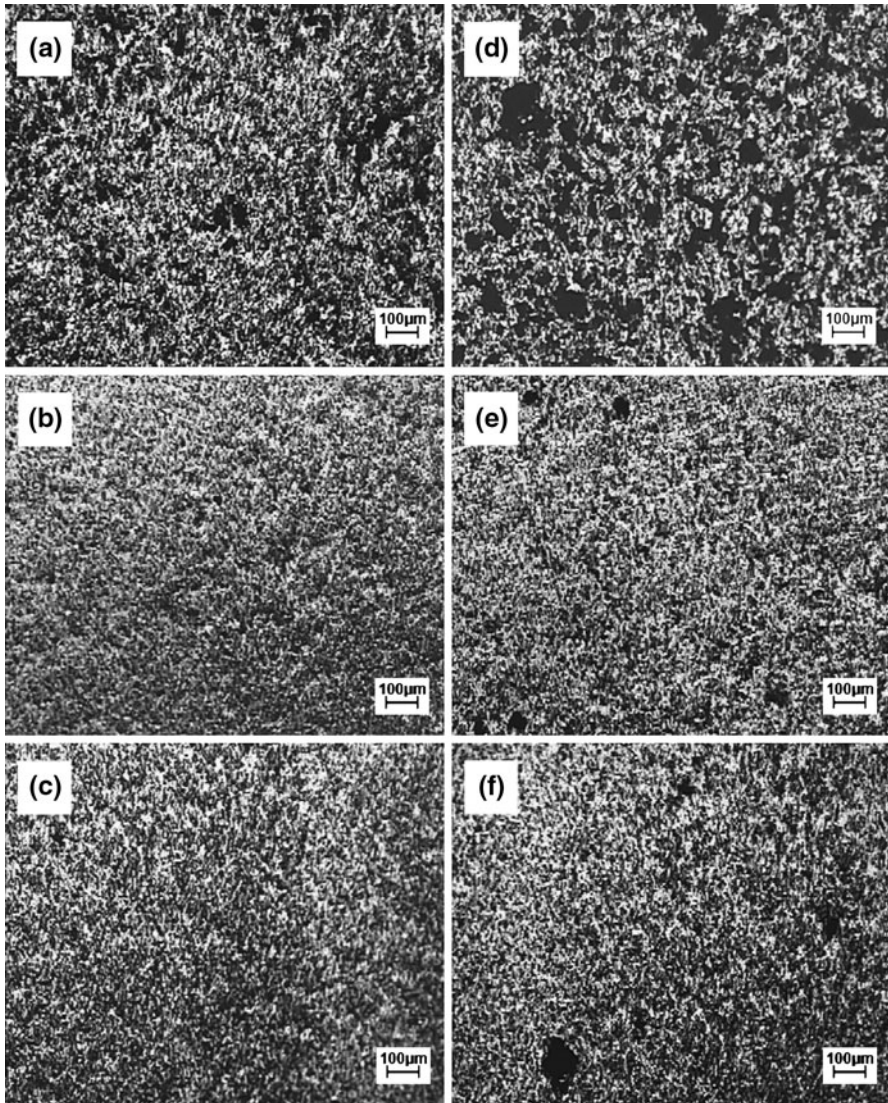


**Fig. 4** Comparison of nanotubes dispersion in PDMS matrix as observed using an optical microscope (transmission mode) for **a** M-PDMS/4 wt% MWCNT-p, **b** M-PDMS/4 wt% MWCNT-OH, **c** M-PDMS/4 wt% MWCNT-COOH, **d** S-PDMS/4 wt% MWCNT-p, **e** S-PDMS/4 wt% MWCNT-OH, and **f** S-PDMS/4 wt% MWCNT-COOH

in PDMS as compared to the pristine MWCNTs (Fig. 4a, d). Only a few nanotubes agglomerates can be seen in composites filled with functionalized nanotubes. In addition, the PDMS/MWCNT-OH and PDMS/MWCNT-COOH composites produced by mini-extruder shows the best nanotubes dispersion as the black-colored spots are equally distributed across the white-colored PDMS area.

## Tensile strength of PDMS/MWCNT composites

Figure 5 shows the tensile strength of PDMS filled with various MWCNTs produced by two different methods. The tensile strength of PDMS/MWCNT composites is highest at 1 wt% loading, regardless of the processing method and fillers used. This indicates that 1 wt% is the optimum nanotube loading within the range of compositions examined here. Further increment of MWCNTs from 2 to 4 wt% resulted in a gradual decrease of tensile strength. However, tensile strength of the composites with functionalized MWCNTs is still higher than those of the neat PDMS. The decline in tensile strength at high filler loading is not unusual [3, 8]. At 4 wt%, the high surface area of nanotubes increased the viscosity of the composite mixture during mixing (see Fig. 5), thus reducing the mixing effectiveness. This led to the formation of large nanotube clusters and agglomerates, which subsequently weakened the composites. SEM micrographs in Fig. 6b, d reveal the presence of large agglomerates in 4 wt% MWCNTs composites. In comparison, Fig. 6a, c shows only a small fraction of agglomerates in 1 wt% MWCNTs composites.

Comparing the composites prepared by the two different processing methods, the tensile strength of composites produced by mini-extruder is much higher than the ones prepared via solution mixing. Taking 1 wt% MWCNTs as example where the tensile strength is the highest, the composites produced by mini-extruder (M-PDMS/MWCNT-p, M-PDMS/MWCNT-OH, and M-PDMS/MWCNT-COOH) exhibited higher tensile strength by 10.38, 16.00, and 5.41 %, respectively, when compared to the solution mixed samples (S-PDMS/MWCNT-p, S-PDMS/MWCNT-OH, and S-PDMS/MWCNT-COOH) at the same filler loading. This result is due to the high shear mixing mechanism of the mini-extruder which produced sufficient

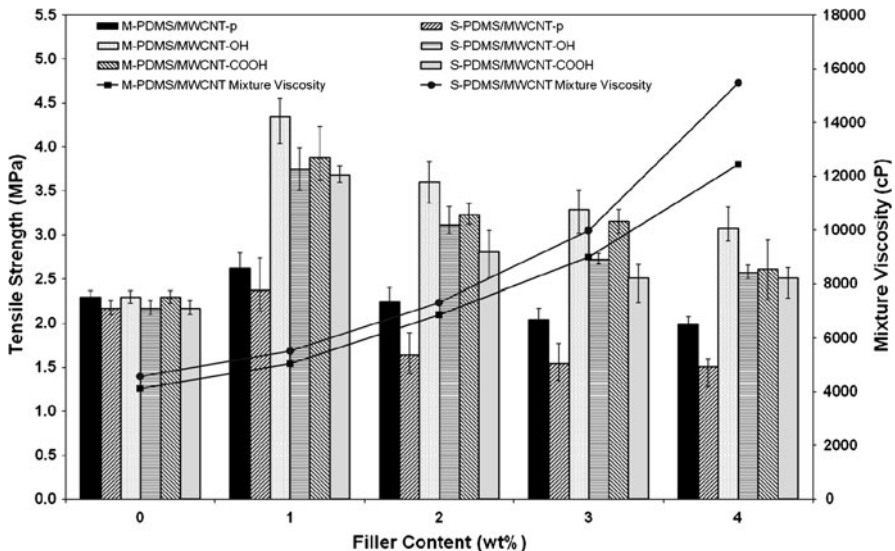


**Fig. 5** Mixture viscosity and tensile strength of PDMS/MWCNT nanocomposites produced by mini-extruder (M-PDMS) and solution mixing (S-PDMS)



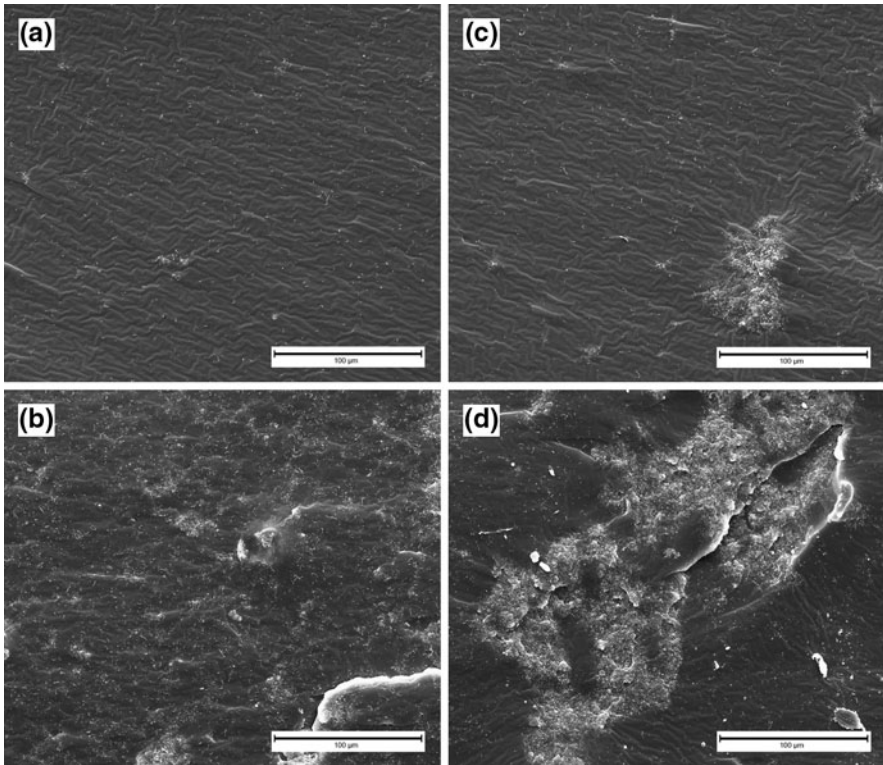


**Fig. 6** SEM micrographs of **a** M-PDMS/1 wt% MWCNT, **b** M-PDMS/4 wt% MWCNT, **c** S-PDMS/1 wt% MWCNT, and **d** S-PDMS/4 wt% MWCNT at  $\times 1,000$  magnification. M-PDMS refers to nanocomposites produced by mini-extruder, while S-PDMS refers to nanocomposites produced via solution mixing

energy to separate and breakdown the bundles of MWCNTs into smaller aggregates and individual nanotubes. In addition, the high shear mixing mechanism of the mini-extruder also reduced the length of the nanotubes, which enabled the nanotubes to be dispersed more easily in the matrix and subsequently increased the tensile strength. SEM observations of the composite fracture surface in Fig. 6 show better nanotube dispersion and smaller aggregates in the mini-extruder-produced composites. In contrast, lumps and large agglomerates of nanotubes, which act as stress concentration point, can be seen in the solution mixed samples. Optical micrographs in Fig. 2 also reveal that the dispersion of nanotubes for composites produced by mini-extruder is better than the ones produced via solution mixing.

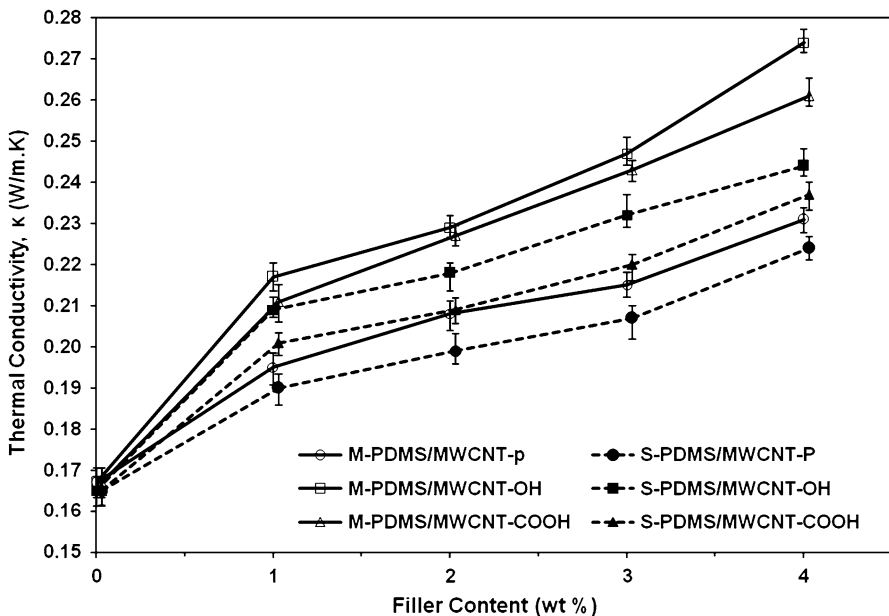
PDMS-filled functionalized MWCNTs shows higher tensile strength than the PDMS-filled pristine MWCNT composites. For example, the tensile strength of 1 wt% M-PDMS/MWCNT-p is 2.62 MPa, whereas the tensile strengths of the systems with 1 wt% M-PDMS/MWCNT-OH and M-PDMS/MWCNT-COOH are 4.35 and 3.88 MPa, respectively. The significantly higher tensile strength in the functionalized systems was due to the hydrogen bonding interaction between the functional group of

MWCNTs and PDMS matrix, which enabled stress transfer to be more effective [8]. It is worth noting that the combination of mini-extruder and MWCNT-OH yields composites with the highest tensile strength.

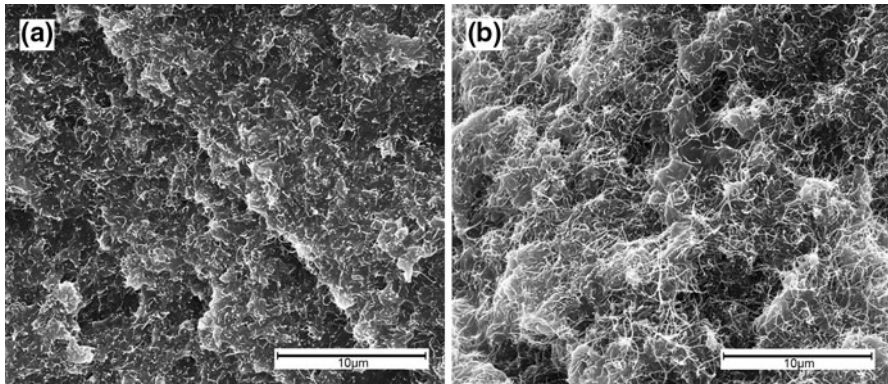
#### Thermal conductivity of PDMS/MWCNT composites

Figure 7 displays the thermal conductivity of PDMS/MWCNT composites at room temperature. The thermal conductivity of all the composites increased with the addition of 1–4 wt% MWCNTs. However, it is noted that the increment is minimal and the thermal conductivity values obtained in the current work are pretty similar to the ones reported in previous works [5, 6, 9], which is  $<1$  W/m.K. In general, the samples produced by mini-extruder are more thermally conductive than the solution mixed samples although the processing method does not affect the thermal conductivity of pure PDMS. For the mini-extruder samples, the addition of 4 wt% MWCNT-OH, MWCNT-COOH, and MWCNT-p into PDMS improves the thermal conductivity by 64, 56, and 38 %, respectively. As for samples produced via solution mixing, the addition of 4 wt% MWCNT-OH, MWCNT-COOH, and MWCNT-p into PDMS increases the thermal conductivity by 46, 42, and 34 %, respectively. Among all the composites tested, the composites produced by mini-extruder and filled with MWCNT-OH have the highest thermal conductivity.

Although thermal conductivity of CNT composite is dominated by phonon vibration and diffusion in the matrix, shorter nanotubes also contribute to the enhancement of thermal conductivity. The enhancement of thermal conductivity in



**Fig. 7** Comparison of thermal conductivity for PDMS/MWCNTs nanocomposites produced by mini-extruder (M-PDMS) and solution mixing (S-PDMS)



**Fig. 8** SEM micrographs of **a** M-PDMS/4 wt% MWCNT-p and **b** S-PDMS/4 wt% MWCNT-p at  $\times 10,000$  comparing the nanotube length

composites with short CNTs may stem from the improved percolation due to better nanotube dispersion [22]. The composites produced by mini-extruder have shorter nanotube length (as shown in Fig. 8) and lower aspect ratio due to the high shear mixing process and these composites have higher thermal conductivity. This is correlated to our results as the mini-extruder produced composites have better dispersed nanotubes, with smaller and lesser agglomerates in comparison to the solution mixed samples, as seen in optical and SEM micrographs in Figs. 4 and 6.

Comparing the composites filled with functionalized fillers, the order of thermal conductivity value from highest to lowest is as follows: PDMS/MWCNT-OH > PDMS/MWCNT-COOH > PDMS/MWCNT-p, indicating that functionalization of nanotubes improves composites thermal conductivity. Functionalization of nanotubes promotes better dispersion of nanotubes in the matrix and improves interfacial heat transport between the polymer matrix and the MWCNTs of which both help to enhance the nanocomposite thermal conductivity [9]. The optical micrographs in Fig. 4 show good nanotubes dispersion in composites filled with functionalized MWCNTs. On the other hand, several large nanotube agglomerates are seen in the composites filled with pristine MWCNTs.

#### Electrical conductivity of PDMS/MWCNTs composites

Figure 9 shows the changes in electrical conductivity of the nanocomposite samples as a function of nanotube content. The conductivity of the solution mixed nanocomposite (S-PDMS/MWCNT-p) increases sharply by five orders of magnitude when 1 wt% nanotube was added. In contrast, the conductivity of the mini-extruder-produced nanocomposite (M-PDMS/MWCNT-p) increased less sharply by three orders of magnitude with 1–3 wt%. The enhancement in electrical conductivity with nanotube content is expected because it obeys the percolation theory [23]. In general, the composites produced by solution mixing method are electrically more conductive than the composites produced by mini-extruder. Theoretically, the electrical conductivity of a filled composite will increase sharply when a conductive

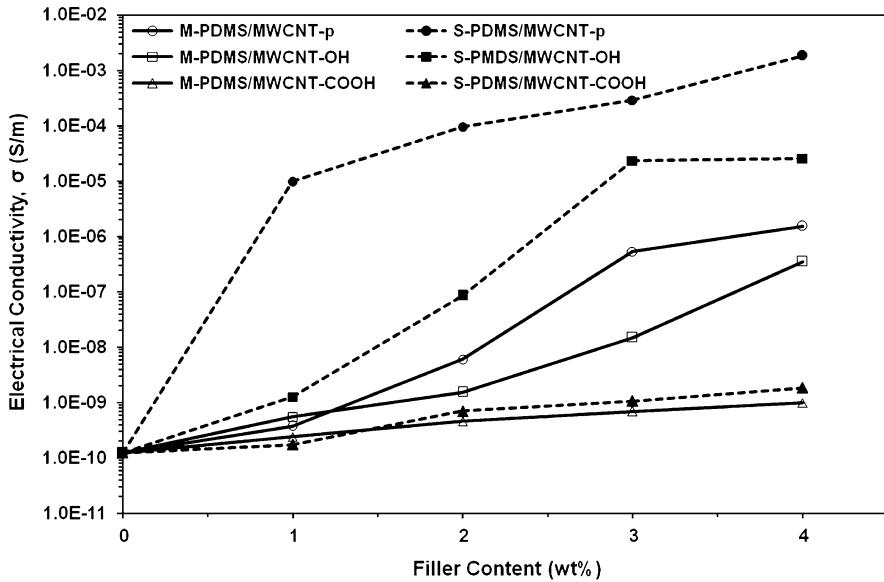


**Fig. 9** Electrical conductivity of PDMS/MWCNT nanocomposite samples as a function of nanotube content for three different fillers produced by mini-extruder (M-PDMS) and solution mixing (S-PDMS)

path of interconnected nanotubes is formed through the volume of the sample. Any parameter that can alter the distance between nanotubes will affect the conductivity [24]. Nanotubes with longer lengths possess higher probability to form interconnected and conductive networks [25]. In this study, the high shear mixing mechanism of the mini-extruder chops the nanotubes to a shorter length; thus, reducing the ability to form a conductive path and network despite an increased dispersion. While there is no specific data to support the reduction of nanotube length and aspect ratio due to difficulty in measuring the length of CNT within a polymer matrix [15]; SEM micrographs in Fig. 8 clearly show that the nanotubes in mini-extruder produced composites are shorter in comparison to the solution mixed composites.

Chemical functionalization can be detrimental to the electrical properties of nanocomposite [26–28]. The electrical conductivity of the PDMS/MWCNT-OH was consistently one to two orders of magnitude lower than that of PDMS/MWCNT-p when nanotubes were loaded from 1 to 4 wt%. Hydroxylation of MWCNTs significantly disrupts the  $\pi$ -conjugation of the outer nanotube layer and reduces the surface electrical conductivity of MWCNTs, leading to a lower electrical conductivity [27]. As for the PDMS/MWCNT-COOH, the electrical conductivity remained nearly invariable, even when the nanocomposite was loaded with filler up to 4 wt%. The insulating behavior of this composite could be due to the processes involved when treating the MWCNTs with carboxyl group. Carboxylated functionalization may cause unbalanced polarization effect and physical structure defects that arise during the acid treatment process [28]. Table 1 shows a comparison of observed electrical conductivity between the present and

**Table 1** Comparison of observed electrical conductivity between present work and previous works

System	Outer diameter (nm)	Processing method	Electrical conductivity (S/m)	Ref.
PDMS/1.5 vol.% MWCNT	<10	Solution mixing	$1.5 \times 10^{-4}$	[5] <sup>a</sup>
PDMS/1.5 vol.% SD-MWCNT	<10	Solution mixing	$3.5 \times 10^{-5}$	
PDMS/4.0 wt% MWCNT	10–20	Solution mixing	$\sim 4.0 \times 10^{-6}$	[20]
PDMS/4.0 wt% MWCNT-OH	10–20	Solution mixing	$\sim 8.0 \times 10^{-8}$	
Epoxy/0.5 wt% MWCNT	10–20	Solution mixing	$\sim 10^{-2}$	[21]
Epoxy/0.5 wt% silane-MWCNT	10–20	Solution mixing	$\sim 10^{-9}$	
PDMS/4.0 wt% MWCNT	40–60	Solution mixing	$1.83 \times 10^{-3}$	Current study
PDMS/4.0 wt% MWCNT-OH	30–50	Solution mixing	$2.53 \times 10^{-5}$	
PDMS/4.0 wt% MWCNT-COOH	30–50	Solution mixing	$1.86 \times 10^{-9}$	
PDMS/4.0 wt% MWCNT	40–60	Mini-extruder	$1.53 \times 10^{-6}$	
PDMS/4.0 wt% MWCNT-OH	30–50	Mini-extruder	$3.54 \times 10^{-7}$	
PDMS/4.0 wt% MWCNT-COOH	30–50	Mini-extruder	$9.86 \times 10^{-10}$	

<sup>a</sup> For comparison purpose, 1.5 vol.% MWCNTs is converted to weight fraction giving a value of 2.1 wt% MWCNT and SD-MWCNT represents silanized diphenyl-carbinol-functionalized MWCNT

previous works [5, 26, 27], of which all the results shows a lower electrical conductivity for functionalized MWCNTs systems as compared to the pristine systems.

### Thermal stability PDMS/MWCNTs composites

The curves in Fig. 10 depict the composite weight change when subjected to high temperature while Table 2 presents the decomposition temperature at 5 % ( $T_5$ ) and 10 % ( $T_{10}$ ) weight loss for PDMS/MWCNT composites produced by different methods. The  $T_5$  of unfilled PDMS produced by mini-extruder and solution mixing are 350 and 354 °C, respectively. The presence of CNT enhances the thermal stability of PMDS composites. Adding 1 wt% of MWCNT shifts the  $T_5$  of the composites higher by 23 °C for the mini-extruder sample and 41 °C for the solution mixed sample. Regardless of the fillers used, the solution mixed composites have higher  $T_5$  and  $T_{10}$  compared to the ones produced by mini-extruder at the same filler content, hinting that these samples were more thermally stable. The  $T_5$  of solution mixed samples are about 10–20 °C higher than the mini-extruder samples. The relatively higher aspect ratio of these nanotubes could have retarded the diffusion and extravasations of small molecules from matrix under high temperature, leading to a heightened decomposition temperature [19, 29].

Functionalization of nanotubes enhances thermal stability of composites, as proven by a few researchers [8, 19, 29]. In this study, both the PDMS/MWCNT-OH and PDMS/MWCNT-COOH composites exhibited higher  $T_5$  and  $T_{10}$  compared to PDMS/MWCNT-p composites. Comparing the composites produced by solution mixing method, the  $T_5$  for S-PDMS/4 wt% MWCNT-OH and S-PDMS/4 wt%



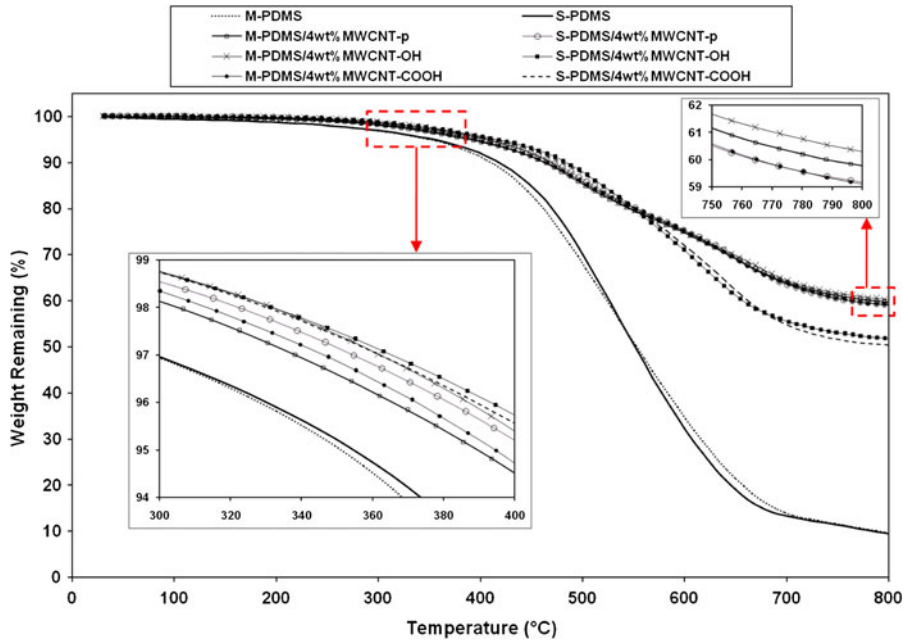


**Fig. 10** TGA curves for nanocomposites produced by mini-extruder (M-PDMS) and solution mixing (S-PDMS)

MWCNT-COOH are 418 and 413 °C, respectively. On the other hand, the  $T_5$  for S-PDMS/4 wt% MWCNT-p is only 404 °C, indicating that thermal decomposition of the composites is retarded by the presence of functionalized CNTs. The hydrogen bonding interaction and good interfacial adhesion between the functionalized CNTs and PDMS matrix restricts the thermal motion of PDMS macromolecules, resulting in a further increase in their thermal stability [29].

## Conclusion

The effects of processing methods on the properties of PDMS/MWCNTs composites were investigated. SEM micrographs of fracture surface reveal that composites produced by mini-extruder have very good and homogenous dispersion as compared to the ones produced by solution mixing; however, this advantage comes at a cost: reduction of nanotube length and aspect ratio. Thus, this processing method only benefits certain properties, such as tensile strength and thermal conductivity. In contrast, the solution mixing method does not heavily damage or reduce the nanotube length, thereby preserving the high aspect ratio of nanotubes. This method does not promote nanotube dispersion as good as that of the former; however, the high aspect ratio of nanotubes compensates the drawback by enhancing the nanocomposite electrical conductivity and thermal stability.

**Table 2** Decomposition temperature of PDMS/MWCNTs nanocomposites

Sample	$T_5$ (°C)		$T_{10}$ (°C)	
	Mini-extruder	Solution mixing	Mini-extruder	Solution mixing
PDMS	350	353	410	418
PDMS/1 wt% MWCNT-p	373	394	452	458
PDMS/4 wt% MWCNT-p	390	404	463	471
PDMS/1 wt% MWCNT-OH	384	404	455	470
PDMS/4 wt% MWCNT-OH	408	418	468	484
PDMS/1 wt% MWCNT-COOH	382	403	455	470
PDMS/4 wt% MWCNT-COOH	395	413	465	481

$T_5$  and  $T_{10}$  refers to decomposition temperatures at 5 % and 10 % weight loss, respectively

Functionalization of MWCNTs with either –OH or –COOH group helps improve interfacial adhesion between MWCNTs and PDMS matrix via a hydrogen bonding interaction, which subsequently improves the tensile strength, thermal conductivity, and thermal stability of the composites. However, the functional groups do not contribute to electrical conductivity enhancement as they disrupt the  $\pi$ -conjugation of the outer nanotube layer and reduce the surface electrical conductivity of MWCNTs. A combination of suitable processing method and surface treatment of MWCNTs can be employed to produce composites with excellent properties. In the current study, the combination of mini-extruder and MWCNT-OH produces composites that possess high tensile strength and high thermal conductivity.

**Acknowledgments** The authors would like to thank the British Council for sponsoring this project via the Prime Minister's Initiative Grant (PMI-2), Grant No. 6050180. The authors also thank Queen Mary University of London (QMUL, UK) for supporting this project. In addition, K. T. S. Kong would like to acknowledge Universiti Sains Malaysia (USM) for providing financial assistance via the USM Fellowship Scheme and Research University Postgraduate Research Grant Scheme (USM-RU-PRGS), Grant No. 8032017.

## References

- Iijima S (1991) Helical microtubules of graphitic carbon. *Nature* 354:56–58
- Thostenson ET, Ren Z, Chou T-W (2001) Advances in the science and technology of carbon nanotubes and their composites: a review. *Compos Sci Technol* 61(13):1899–1912. doi:10.1016/S0266-3538(01)00094-X
- Zhou Z, Wang S, Lu L, Zhang Y, Zhang Y (2008) Functionalization of multi-wall carbon nanotubes with silane and its reinforcement on polypropylene composites. *Compos Sci Technol* 68(7–8): 1727–1733. doi:10.1016/j.compscitech.2008.02.003
- Sandler J, Shaffer MSP, Prasse T, Bauhofer W, Schulte K, Windle AH (1999) Development of a dispersion process for carbon nanotubes in an epoxy matrix and the resulting electrical properties. *Polymer* 40(21):5967–5971. doi:10.1016/S0032-3861(99)00166-4
- Chua TP, Mariatti M, Azizan A, Rashid AA (2010) Effects of surface-functionalized multi-walled carbon nanotubes on the properties of poly(dimethyl siloxane) nanocomposites. *Compos Sci Technol* 70(4):671–677. doi:10.1016/j.compscitech.2009.12.023

6. Hong J, Lee J, Hong CK, Shim SE (2010) Effect of dispersion state of carbon nanotube on the thermal conductivity of poly(dimethyl siloxane) composites. *Curr Appl Phys* 10(1):359–363. doi:[10.1016/j.cap.2009.06.028](https://doi.org/10.1016/j.cap.2009.06.028)
7. Wu C-L, Lin H-C, Hsu J-S, Yip M-C, Fang W (2009) Static and dynamic mechanical properties of polydimethylsiloxane/carbon nanotube nanocomposites. *Thin Solid Films* 517(17):4895–4901. doi:[10.1016/j.tsf.2009.03.146](https://doi.org/10.1016/j.tsf.2009.03.146)
8. Chen X, Wang J, Lin M, Zhong W, Feng T, Chen J, Xue F (2008) Mechanical and thermal properties of epoxy nanocomposites reinforced with amino-functionalized multi-walled carbon nanotubes. *Mater Sci Eng A* 492(1–2):236–242. doi:[10.1016/j.msea.2008.04.044](https://doi.org/10.1016/j.msea.2008.04.044)
9. Yang K, Gu M, Guo Y, Pan X, Mu G (2009) Effects of carbon nanotube functionalization on the mechanical and thermal properties of epoxy composites. *Carbon* 47(7):1723–1737. doi:[10.1016/j.carbon.2009.02.029](https://doi.org/10.1016/j.carbon.2009.02.029)
10. Wang Z, Ciselli P, Peijs T (2007) The extraordinary reinforcing efficiency of single-walled carbon nanotubes in oriented poly(vinyl alcohol) tapes. *Nanotechnology* 18(45):455709. doi:[10.1088/0957-4484/18/45/455709](https://doi.org/10.1088/0957-4484/18/45/455709)
11. Deng H, Bilotti E, Zhang R, Peijs T (2010) Effective reinforcement of carbon nanotubes in polypropylene matrices. *J Appl Polym Sci* 118(1):30–41. doi:[10.1002/app.30783](https://doi.org/10.1002/app.30783)
12. Kathi J, Rhee K-Y, Lee JH (2009) Effect of chemical functionalization of multi-walled carbon nanotubes with 3-aminopropyltriethoxysilane on mechanical and morphological properties of epoxy nanocomposites. *Compos A* 40(6–7):800–809
13. Lee Y (2003) Surface properties of fluorinated single-walled carbon nanotubes. *J Fluorine Chem* 120(2):99–104. doi:[10.1016/s0022-1139\(02\)00316-0](https://doi.org/10.1016/s0022-1139(02)00316-0)
14. Kim YJ, Shin TS, Choi HD, Kwon JH, Chung Y-C, Yoon HG (2005) Electrical conductivity of chemically modified multiwalled carbon nanotube/epoxy composites. *Carbon* 43(1):23–30. doi:[10.1016/j.carbon.2004.08.015](https://doi.org/10.1016/j.carbon.2004.08.015)
15. Li J, Ma PC, Chow WS, To CK, Tang BZ, Kim J-K (2007) Correlations between percolation threshold, dispersion state, and aspect ratio of carbon nanotubes. *Adv Funct Mater* 17(16):3207–3215. doi:[10.1002/adfm.200700065](https://doi.org/10.1002/adfm.200700065)
16. Song YS, Youn JR (2005) Influence of dispersion states of carbon nanotubes on physical properties of epoxy nanocomposites. *Carbon* 43(7):1378–1385. doi:[10.1016/j.carbon.2005.01.007](https://doi.org/10.1016/j.carbon.2005.01.007)
17. Spitalsky Z, Tasis D, Papagelis K, Galiotis C (2010) Carbon nanotube–polymer composites: chemistry, processing, mechanical and electrical properties. *Prog Polym Sci* 35(3):357–401. doi:[10.1016/j.progpolymsci.2009.09.003](https://doi.org/10.1016/j.progpolymsci.2009.09.003)
18. Xing Y, Li L, Chusuei CC, Hull RV (2005) Sonochemical oxidation of multiwalled carbon nanotubes. *Langmuir* 21(9):4185–4190. doi:[10.1021/la047268e](https://doi.org/10.1021/la047268e)
19. Kim JY (2009) Carbon nanotube-reinforced thermotropic liquid crystal polymer nanocomposites. *Materials* 2(4):1955–1974. doi:[10.3390/ma2041955](https://doi.org/10.3390/ma2041955)
20. Bandarian M, Shojaei A, Rashidi AM (2011) Thermal, mechanical and acoustic damping properties of flexible open-cell polyurethane/multi-walled carbon nanotube foams: effect of surface functionality of nanotubes. *Polym Int* 60(3):475–482
21. Song P, Xu L, Guo Z, Zhang Y, Fan Z (2008) Flame-retardant-wrapped carbon nanotubes for simultaneously improving the flame retardancy and mechanical properties of polypropylene. *J Mater Chem* 18(42):5083–5091
22. Wang S, Liang R, Wang B, Zhang C (2009) Dispersion and thermal conductivity of carbon nanotube composites. *Carbon* 47(1):53–57. doi:[10.1016/j.carbon.2008.08.024](https://doi.org/10.1016/j.carbon.2008.08.024)
23. Last BJ, Thouless DJ (1971) Percolation theory and electrical conductivity. *Phys Rev Lett* 27(25):1719
24. Ciselli P, Lu L, Busfield JJC, Peijs T (2010) Piezoresistive polymer composites based on EPDM and MWNTs for strain sensing applications. *e-Polymers* 14
25. Bai J, Allaoui A (2003) Effect of the length and the aggregate size of MWNTs on the improvement efficiency of the mechanical and electrical properties of nanocomposites—experimental investigation. *Compos A* 34(8):689–694. doi:[10.1016/s1359-835x\(03\)00140-4](https://doi.org/10.1016/s1359-835x(03)00140-4)
26. Gojny FH, Wichmann MHG, Fiedler B, Kinloch IA, Bauhofer W, Windle AH, Schulte K (2006) Evaluation and identification of electrical and thermal conduction mechanisms in carbon nanotube/epoxy composites. *Polymer* 47(6):2036–2045. doi:[10.1016/j.polymer.2006.01.029](https://doi.org/10.1016/j.polymer.2006.01.029)
27. Kohlmeyer RR, Javadi A, Pradhan B, Pilla S, Setyowati K, Chen J, Gong S (2009) Electrical and dielectric properties of hydroxylated carbon nanotube–elastomer composites. *J Phys Chem C* 113(41):17626–17629. doi:[10.1021/jp901082c](https://doi.org/10.1021/jp901082c)

28. Sulong AB, Muhamad N, Sahari J, Ramli R, Deros BM, Park J (2009) Electrical conductivity behavior of chemical functionalized MWCNTs epoxy nanocomposites. *Eur J Scientific Res* 29(1): 13–21
29. Wang J, Fang Z, Gu A, Xu L, Liu F (2006) Effect of amino-functionalization of multi-walled carbon nanotubes on the dispersion with epoxy resin matrix. *J Appl Polym Sci* 100(1):97–104. doi: [10.1002/app.22647](https://doi.org/10.1002/app.22647)